



PII S00167037(99)00325-7

Neodymium isotopic study of rare earth element sources and mobility in hydrothermal Fe oxide (Fe-P-REE) systems

JAMES D. GLEASON,^{*,†} MARK A. MARIKOS, MARK D. BARTON, and DAVID A. JOHNSON

University of Arizona, Department of Geosciences, Tucson, Arizona 85721, USA

(Received November 26, 1997; accepted in revised form August 2, 1999)

Abstract—Rare earth element (REE)-enriched, igneous-related hydrothermal Fe-oxide hosted (Fe-P-REE) systems from four areas in North America have been analyzed for their neodymium isotopic composition to constrain REE sources and mobility in these systems. The Nd isotopic results evidence a common pattern of REE concentration from igneous sources despite large differences in age (Proterozoic to Tertiary), tectonic setting (subduction vs. intraplate), and magmatic style (mafic vs. felsic).

In the Middle Proterozoic St. Francois Mountains terrane of southeastern Missouri, ϵ_{Nd} for Fe-P-REE (apatite, monazite, xenotime) deposits ranges from +3.5 to +5.1, similar to associated felsic to intermediate igneous rocks of the same age ($\epsilon_{Nd} = +2.6$ to +6.2). At the mid-Jurassic Humboldt mafic complex in western Nevada, ϵ_{Nd} for Fe-P-REE (apatite) mineralization varies between +1.1 and +2.4, similar to associated mafic igneous rocks (−1.0 to +3.5). In the nearby Cortez Mountains in central Nevada, mid-Jurassic felsic volcanic and plutonic rocks ($\epsilon_{Nd} = -2.0$ to −4.4) are associated with Fe-P-REE (apatite–monazite) mineralization having similar ϵ_{Nd} (−1.7 to −2.4). At Cerro de Mercado, Durango, Mexico, all assemblages analyzed in this Tertiary rhyolite-hosted Fe oxide deposit have identical isotopic compositions with $\epsilon_{Nd} = -2.5$. These data are consistent with coeval igneous host rocks being the primary source of REE in all four regions, and are inconsistent with a significant contribution of REE from other sources. Interpretations of the origin of these hydrothermal systems and their concomitant REE mobility must account for nonspecialized igneous sources and varied tectonic settings. Copyright © 2000 Elsevier Science Ltd

1. INTRODUCTION

Hydrothermal fluids are central to the genesis of many rare earth element (REE)-rich, Fe oxide-hosted (Fe-P-REE) mineral deposits worldwide, including the large economic deposits at Olympic Dam, Australia, and the Kiruna Iron District in northern Sweden (e.g., Oreskes and Einaudi, 1990; Hitzman et al., 1992; Gow et al., 1994; Foose and McLelland, 1995; Haynes et al., 1995; Barton and Johnson, 1996). These deposits can have REE enrichments that are 5–50 times that of associated rocks typically because of their elevated phosphate contents (e.g., Oreskes and Einaudi, 1990; Frietsch and Perdahl, 1995). The sources of the REE in these hydrothermal systems, and the conditions necessary for mobilizing, concentrating, and precipitating REE on a large scale remain poorly understood (e.g., Einaudi and Oreskes, 1990; Barton and Johnson, 1996). For this reason several groups, including ours, have been obtaining Sm–Nd isotopic data for a variety of Fe-P-REE mineral deposits in an effort to track REE sources and pathways (e.g., Johnson and Cross, 1991; Marikos and Barton, 1993; Johnson and McCulloch, 1995).

In this article, we report new Nd isotopic data on REE-rich phosphates, Fe-oxide minerals, and associated fresh and altered igneous rocks from four well-characterized Fe-oxide districts in North America, ranging in age from Proterozoic to Tertiary (Fig. 1). In the St. Francois Mountains of southeastern Missouri, Middle Proterozoic (≈ 1.47 Ga) volcanic rocks of the

mid-continent granite–rhyolite terrane host locally high-grade REE ore associated with numerous Fe oxide-rich deposits (e.g., Marikos et al., 1990; Nuelle et al., 1992; Sidder et al., 1993). Jurassic (≈ 165 Ma) hydrothermal alteration and associated Fe-P-REE mineralization is extensively developed and well exposed in the Humboldt mafic complex of western Nevada and the Cortez Mountains felsic volcanic–plutonic suite of central Nevada (Barton et al., 1993; Battles and Barton, 1995). Youngest of the four at about 30 Ma is Cerro de Mercado, Durango, Mexico, where Fe oxide mineralization is associated with a felsic volcanic center on the eastern flank of the Sierra Madre Occidental (Lyons, 1988). Our data are consistent with dominantly igneous host sources for the REE at all four localities, regardless of host lithology, age, or tectonic setting. These data, in conjunction with ongoing field and geochemical studies, imply common processes whereby the REE and other metals are sourced from hot igneous rocks, moved by large-scale hydrothermal fluid circulation, and precipitated in more concentrated REE- and Fe oxide-rich mineral deposits. These kinds of observations do not resolve the ultimate sources of fluids (both magmatic and nonmagmatic brines could be involved); however, if contrasting igneous sources of solutes can be demonstrated, then nonmagmatic fluid sources provide the simplest explanation for the overall characteristics of these deposits (Barton and Johnson, 1996).

2. GEOLOGIC SETTING OF FE OXIDE DEPOSITS

2.1. St. Francois Mountains, Southeast Missouri

Middle Proterozoic (1.46 Ga) rhyolites and related igneous rocks of the St. Francois Mountains in southeast Missouri (Fig. 1) are associated with several apatite-bearing Fe oxide deposits

*Author to whom correspondence should be addressed (jgleason@gammal.lpl.arizona.edu).

†Present address: University of Arizona, Lunar and Planetary Laboratory, Tucson, AZ 85721.

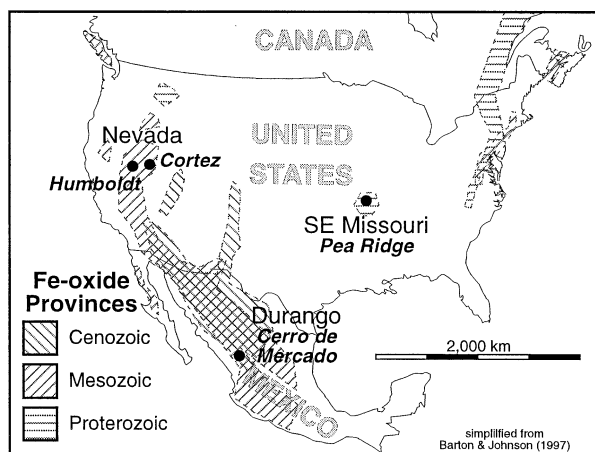


Fig. 1. Locality map showing the Fe oxide-rich hydrothermal systems studied here including the St. Francois Mountains (Missouri), the Humboldt mafic complex and Cortez Mountains (Nevada), and Cerro de Mercado (Durango). Also illustrated is the general distribution of similar systems of Proterozoic, Mesozoic, and Tertiary age.

that locally contain high grade (>10 wt.% REE_2O_3) REE ores (e.g., Kisvarsanyi, 1990; Marikos et al., 1990; Sims, 1990; Nuelle et al., 1992; Sidder et al., 1993). Magnetite mineralization is best developed in elongate, cross-cutting tabular bodies associated with rhyolite flows, and appears to be nearly coeval with host igneous rocks, based on cross-cutting relations (Seeger et al., 1989; Marikos et al., 1990; Day et al., 1991; Nuelle et al., 1992; Sidder et al., 1993). REE-rich breccia pipes cross-cut the zoned magnetite-apatite deposit at the Pea Ridge mine where the most extensive studies have been carried out (Seeger et al., 1989; Marikos et al., 1990; Day et al., 1991; Nuelle et al., 1992; Sidder et al., 1993), and where direct comparisons have been made to the high grade, Fe oxide-associated REE deposits at Olympic Dam, Australia (e.g., Einaudi and Oreskes, 1990; Marikos et al., 1990). At Pea Ridge, complex igneous-related hydrothermal processes produced early magnetite mineralization overprinted by hematitic alteration, followed by late-stage emplacement of the breccia pipes that host monazite-rich REE ore (Seeger et al., 1989; Marikos et al., 1990; Day et al., 1991; Nuelle et al., 1992; Sidder et al., 1993). Previous workers (Seeger et al., 1989; Day et al., 1991; Nuelle et al., 1992; Sidder et al., 1993) interpreted the breccia pipes to have formed from magmatically derived hydrothermal fluids localized along faults and lithologic contacts within the magnetite body. A U-Pb date of 1.466 ± 0.004 Ga on xenotime from a late cross-cutting quartz vein (Van Schmus et al., 1996) associated with one of the breccia pipes at Pea Ridge, and a U-Pb age of 1.473 ± 0.003 (Van Schmus et al., 1996) for a host rhyolite at Pea Ridge, supports earlier conclusions that the Fe oxide REE mineralization is coeval with regional magmatism in the St. Francois Mountains.

2.2. Humboldt Mafic Complex and Cortez Mountains, Nevada

The Jurassic (≈ 165 Ma) Humboldt mafic complex in western Nevada and the roughly coeval felsic rocks of the nearby

Cortez Mountains (Fig. 1), belong to a broad belt of early to middle Mesozoic igneous-related sodium-rich hydrothermal alteration and associated Fe oxide-rich mineralization within the Basin and Range Province of the western United States (Barton et al., 1988; Battles and Barton, 1995). In both areas, large intrusive complexes were emplaced into late Paleozoic to early Mesozoic sedimentary sequences and into their own extensive volcanic carapaces. Intensely sodically altered (scapolitized) mafic volcanic and hypabyssal rocks of the 500 km² Humboldt composite intrusive-extrusive complex (Speed, 1976), and extensively sodically altered (albitized) and potassically altered (K-mica, K-feldspar) felsic volcanic and plutonic rocks of the Cortez Mountains (Muffler, 1964), host a variety of Fe-P-REE deposits that we (e.g., Johnson et al., 1993) interpret to be hydrothermal in origin based on new mapping, petrological, and light stable isotopic investigations. Saline fluid inclusions, the volume of alkali-rich alteration, and clearly nonmagmatic stable isotope signatures ($\delta^{18}\text{O}$ calculated for waters is significantly higher than magmatic values) in the hydrothermal alteration lead us to believe that the Humboldt and Cortez systems involved brines of evaporitic or connate origin (Battles and Barton, 1995; Barton and Johnson, 1996; 1997).

At both localities, the bulk of the REE are contained in hydrothermal apatites associated with massive magnetite and hematite bodies (Johnson et al., 1995). Cross-cutting magnetite-rich apatite-bearing bodies with hematitic overprint occur in both areas and are thought to represent the deepest exposed levels of hydrothermal mineralization. Overall REE concentration levels and degrees of LREE enrichment (e.g., La/Yb) are higher at Cortez than in the Humboldt Fe-P-REE deposits, reflecting the more felsic, enriched nature of the host igneous rocks in the Cortez Mountains suite. Mass balance relationships in these systems are consistent with REE and other metals having been leached from hot igneous host rocks by circulating Na-rich fluids and redeposited as Fe-P-REE-rich phosphates (Johnson and Barton, 1997).

2.3. Cerro de Mercado, Durango, Mexico

Tertiary (30 Ma) apatite-bearing iron deposits at Cerro de Mercado in the state of Durango, Mexico (Fig. 1), are associated with felsic volcanic rocks of the Chupaderos caldera within the Sierra Madre Occidental volcanic province (Lyons, 1988). Lyons (1988) interpreted these iron deposits, which include stratabound magnetite and hematite-rich facies, to have formed by largely volcanic processes, producing a variety of volcanic, intrusive, replacement, and sedimentary textures. Field relationships, an abundance of hydrothermal features, and many geochemical similarities to other similar types of Fe-P-REE deposits worldwide have led other investigators (e.g., Labarthe-Hernandez et al., 1987) to conclude that they are primarily hydrothermal replacement deposits. REE at Cerro de Mercado are mainly hosted by fluorapatite, which occurs intergrown with Fe oxide (martite, pseudomorphs after magnetite), lining cavities, fractures, and bedding planes within the main ore body (Lyons, 1988). As in the other deposits studied here, the REE reach higher concentrations in paragenetically late apatite.

Table 1. Sm-Nd isotopic data for the St. Francois Mountains.

Sample	Material	Sm (ppm)	Nd (ppm)	$^{147}\text{Sm}/^{144}\text{Nd}^a$	$^{143}\text{Nd}/^{144}\text{Nd}^b$ (measured)	ϵ_{Nd}^c (1.46 Ga)
<i>Pea Ridge</i>						
88PR020	Aplite/host ign.	11.60	54.10	0.1292	0.512230 ± 7	+4.7
90PR004	Diabase/late ign.	3.41	9.96	0.2069	0.513071 ± 8	+6.5
	Duplicate	3.46	10.11	0.2067	0.513051 ± 7	+6.2
90PR044	Rhyodacite/host ign.	9.60	47.90	0.1218	0.512110 ± 5	+3.8
90PR052	Rhyolite/host ign.	7.90	39.90	0.1234	0.512158 ± 7	+4.4
90PR053	REE breccia/ore	1857	10908	0.1029	0.511964 ± 8	+4.5
88PR999	Early apatite/REE min.	555.7	3342	0.1005	0.511913 ± 5	+3.9
88PR120	Late apatite/REE min.	454.7	2781	0.0988	0.511874 ± 8	+3.5
88PR118	Xenotime/REE min.	5767	6493	0.5374	0.516181 ± 6	+5.1
88PR26	Hematite/ore	9.76	55.34	0.1066	0.511952 ± 11	+3.6
90PR012	Early magnetite/ore	8.39	34.55	0.1467	0.512327 ± 7	+3.3
90PR023	Quartz-actinolite/ore	15.90	50.70	0.1899	0.512783 ± 7	+4.1
<i>Iron Mt.</i>						
931MA	Actinolite sep/ore	11.58	47.05	0.1488	0.512373 ± 7	+3.9
931MG	Garnet sep/ore	3.80	16.06	0.1431	0.512332 ± 5	+4.1
	Duplicate	3.95	16.59	0.1440	0.512338 ± 6	+4.1
IM3948	Andesite/host ign.	5.79	25.75	0.1359	0.512256 ± 8	+4.0
<i>Pilot Knob</i>						
PKPIPE	Barite breccia/ore	1.21	5.42	0.1345	0.512130 ± 7	+1.8
PKSURF	Bedded hematite Formation/ore	0.59	6.11	0.0580	0.511446 ± 15	+2.8
<i>Boss-Bixby</i>						
J17SILL	Granite/host	8.26	37.94	0.1317	0.512146 ± 9	+2.6
J17syen	K-fenite/alt.	7.84	38.89	0.1218	0.512073 ± 6	+3.3
<i>Floyd Twr.</i>						
88FT920	Magnetite trachyte	10.80	50.60	0.1294	0.512140 ± 8	+2.9
WA11-1256	Trachybasalt/ign.	4.50	18.60	0.1446	0.512321 ± 5	+3.6
<i>Basement</i>						
GE1	Orthogneiss	7.90	47.40	0.1014	0.511696 ± 6	-0.5
L3-1713	Paragneiss	9.30	47.30	0.1188	0.511893 ± 5	+0.1

^a Uncertainties in $^{147}\text{Sm}/^{144}\text{Nd} < 0.5\%$.

[†] Isotopic ratios normalized to $^{146}\text{Nd}/^{144}\text{Nd} = 0.7219$. Stated uncertainties reflect in-run precision (in ppm) and not reproducibility.

^c $\epsilon_{\text{Nd}} = 10^4 [(^{143}\text{Nd}/^{144}\text{Nd})_{(\text{sample})} / (^{143}\text{Nd}/^{144}\text{Nd})_{(\text{CHUR})} - 1]$, calculated using $^{143}\text{Nd}/^{144}\text{Nd} = 0.512638$ as present day CHUR value and $^{147}\text{Sm}/^{147}\text{Nd}_{\text{CHUR}} = 0.1966$, where $t = 1465$ Ma.

Analyst: M. Marikos

3. METHODS

Representative samples of altered and fresh igneous rocks, associated hydrothermal REE-rich phosphate minerals, and host Fe oxide deposits from all four localities were analyzed for their Nd isotopic composition. Where available, several generations of REE-mineralized materials were sampled in an attempt to discover any spatial and temporal variations in Nd isotopic compositions that might have developed as these systems evolved. Before analysis, whole rock samples were cleaned in deionized water, crushed in a steel jaw crusher, and powdered in a shatterbox using an aluminum oxide mill. Mineral separates were ground into powder using a boron carbide mortar. Laboratory methods followed those of Patchett and Ruiz (1987). Overnight hot plate dissolution (9:1 HF/HNO₃) in open bombs was followed by hydrothermal oven dissolution (9:1 HF/HNO₃) in sealed high-pressure bombs for 7 days at 160°C. All samples were treated with HClO₄ to drive off fluorides and then redissolved in 6 M HCl. A ^{149}Sm - ^{150}Nd tracer solution was combined with each sample, and the mixture was warmed for several hours on a hotplate in a large volume of 6 M HCl to ensure complete spike-sample equilibration. Sm and Nd were separated by conventional ion exchange methods and run on a fully automated VG-354 multicollector mass spectrometer at the University of Arizona following the procedures described by Patchett and Ruiz (1987). During the period of this study (1991–1994), the La Jolla Nd isotopic standard gave $^{143}\text{Nd}/^{144}\text{Nd} = 0.511867 \pm 12$; $\epsilon_{\text{Nd}} = -15.0 \pm 0.23$ ($n = 28$), and laboratory blanks averaged <100 pg Sm and <200 pg Nd.

4. RESULTS

4.1. St. Francois Mountains

Fresh and altered igneous host rocks, REE-bearing breccias and mineral separates, and associated Fe oxides from several localities in the St. Francois Mountains were analyzed for their Nd isotopic composition (see Appendix 1 for sample descriptions and localities). Results are given in Table 1. Most samples are from the Pea Ridge mine (described in section 2.1 and below), where geologic relations are best known. A number of samples from other mineralized localities in the St. Francois terrane were also analyzed for comparison. District-wide, initial ϵ_{Nd} values (at 1.46 Ga) for fresh host igneous rocks vary between +2.6 and +6.2, Fe oxide and related alteration mineral assemblages vary between +1.8 and +4.1, and REE-rich breccias and phosphate mineral separates vary between +3.5 to +5.1 (Fig. 2A).

At the Pea Ridge mine (Fig. 3), where REE reach their highest concentrations in breccia pipes that cross-cut the main magnetite ore body (Table 1), ϵ_{Nd} values for rhyolitic host rock vary from +3.8 to +4.4. Late cross-cutting aplite and diabase dikes, which postdate the ore body, have ϵ_{Nd} values of +4.7 and +6.2, respectively. A sample of quartz-rich amphibole-

Table 2. Sm-Nd isotopic data for the Humboldt, Cortez and Cerro de Mercado.

Sample	Material	Sm (ppm)	Nd (ppm)	$^{147}\text{Sm}/^{144}\text{Nd}^a$	$^{143}\text{Nd}/^{144}\text{Nd}^b$ (measured)	ϵ_{Nd}^c (initial)
<i>Humboldt</i>						
Hm91-G-Ap	Apatite/REE min.	163.9	1055	0.0939	0.512645 ± 6	+2.3
Hm92-6h	Picrite/host igneous	1.92	8.07	0.1440	0.512541 ± 5	-0.8
	Duplicate	2.06	8.65	0.1440	0.512530 ± 7	-1.0
Hm94-1g	Albitized basalt/alt.	4.78	23.60	0.1225	0.512650 ± 5	+1.8
Hm93-11a'	Gabbro/host igneous	3.45	14.84	0.1407	0.512755 ± 5	+3.5
Hm93-16t	Late Fe-oxide/ore	1.09	8.78	0.0755	0.512578 ± 6	+1.4
TrJ89-6b	Albitized gabbro/alt.	23.13	162.22	0.0862	0.512642 ± 6	+2.4
TrJ89-7c	Scapolite/alt.	1.28	7.43	0.1042	0.512661 ± 5	+2.4
TrJ89-7f	Apatite/REE min.	162.56	927.88	0.1058	0.512664 ± 6	+2.4
TrJ90-1c	Late calcite-apatite	35.77	169.33	0.1277	0.512620 ± 6	+1.1
TrJ90-13A	Albitized dike/alt.	3.09	13.77	0.1356	0.512662 ± 6	+1.8
<i>Cortez</i>						
CM90-1G'	Jasper/late REE min.	29.92	256.36	0.0706	0.512415 ± 5	-1.7
CM90-1A	Rhyolite/host ign.	8.72	52.49	0.1005	0.512395 ± 6	-2.7
CM92-3f	Granite/host igneous	2.97	13.55	0.1327	0.512342 ± 6	-4.4
CM92-4a	Diorite/host igneous	4.04	19.53	0.1134	0.512441 ± 6	-2.1
CM92-6p	Apatite/REE min.	619.5	4869	0.0769	0.512408 ± 7	-2.0
CM92-1g	Andesite/host igneous	5.61	34.28	0.0989	0.512429 ± 8	-2.0
CM92-6m	Apatite/REE min.	31.63	255.2	0.0749	0.512382 ± 10	-2.4
<i>Durango</i>						
D93-3n'	Apatite/REE min.	244.3	1696	0.0871	0.512490 ± 8	-2.5
D94-3a	Apatite/REE min.	160.8	1305	0.0744	0.512477 ± 13	-2.7
D94-4a	Rhyolite/host igneous	17.71	88.02	0.1216	0.512511 ± 9	-2.2
D94-4t	Gypsum-Fe-ox/ore	0.874	5.98	0.0882	0.512499 ± 8	-2.2

^a Uncertainties in $^{147}\text{Sm}/^{144}\text{Nd} < 0.5\%$.

^b Isotopic ratios normalized to $^{146}\text{Nd}/^{144}\text{Nd} = 0.7219$. Stated uncertainties reflect in-run precision (in ppm) and not reproducibility.

^c $\epsilon_{\text{Nd}} = 10^4 [(^{143}\text{Nd}/^{144}\text{Nd})_{(\text{sample})} / (^{143}\text{Nd}/^{144}\text{Nd})_{(\text{CHUR})} - 1]$, calculated using $^{143}\text{Nd}/^{144}\text{Nd} = 0.512638$ as present day CHUR value and $^{147}\text{Sm}/^{147}\text{Nd}_{\text{CHUR}} = 0.1966$, where $t = 165$ Ma (Humboldt-Cortez) and 30 Ma (Cerro).

Analysts: J. Gleason and M. Marikos

bearing skarn (altered rhyolite) which predates the main magnetite ore body (Nuelle et al., 1992; Sidder et al., 1993) has an ϵ_{Nd} of +4.1 (Table 1). Massive magnetite from the main ore body has an ϵ_{Nd} of +3.3, whereas fluorapatite, which is present in amounts up to 10% within the magnetite zone as interstitial grains, pods, and vug-lining gangue material (Nuelle et al., 1992; Sidder et al., 1993), has an ϵ_{Nd} of +3.9. Specular hematite postdating the massive magnetite (Nuelle et al., 1992; Sidder et al., 1993) has an ϵ_{Nd} of +3.5. Silicification and associated potassic alteration of rhyolitic wall rock hosting the ore body postdates hematite formation, and is thought to be partly contemporaneous with emplacement of the REE-rich breccia pipes (Nuelle et al., 1992; Sidder et al., 1993). Xenotime and apatite (dated at 1.46 Ga by U-Pb methods; Van Schmus et al., 1996) from late cross-cutting quartz veins associated with the silicified zone have ϵ_{Nd} of +5.1 and +3.5, respectively, whereas a sample of monazite-bearing REE-rich breccia has an ϵ_{Nd} of +4.5.

Samples analyzed from other parts of the region include unaltered igneous rocks, Fe oxide minerals, and skarn rocks, including quartz-rich garnet- and actinolite-bearing assemblages representing altered igneous host lithologies. At Iron Mountain, actinolite and garnet mineral separates from a quartz-rich calc-silicate alteration zone associated with the magnetite ore body yield ϵ_{Nd} values of +3.9 and +4.1, respectively, identical to unaltered Iron Mountain andesite that hosts this mineralization ($\epsilon_{\text{Nd}} = +4.0$). Bedded hematite and a non-REE-rich, barite-bearing breccia from Pilot Knob have ϵ_{Nd} values of +1.8 and +2.8, respectively. At the Boss-Bixby

mine, unaltered granite has an ϵ_{Nd} of +2.6, whereas a sample of the K-syenite stock (K-metasomatized granite) that hosts the mineralization (Kisvarsanyi, 1990) has an ϵ_{Nd} of +3.3. At Floyd Tower, magnetite-bearing trachytes from ring intrusions associated with the Pea Ridge caldera complex (Kisvarsanyi, 1990) have ϵ_{Nd} values ranging from +2.9 to +3.6. Two samples of 1.65-Ga basement gneiss recovered from drill cores in the region (Van Schmus et al., 1996) have ϵ_{Nd} values of +2.1 and +2.2 at 1.46 Ga.

At the Pea Ridge mine, deposits bracketed in time between rhyolite host rocks and cross-cutting mafic and felsic dikes (amphibole-quartz, magnetite and hematite zones) form an isotopically coherent group (average $\epsilon_{\text{Nd}} = +3.7$) trending toward values only slightly more negative than the host rhyolite (average $\epsilon_{\text{Nd}} = +4.1$). These early assemblages were deposited at higher temperatures ($\approx 680^\circ\text{C}$) than the later, REE-rich breccia pipes ($\approx 300^\circ\text{C}$), based on the oxygen isotope and fluid inclusion data of Sidder et al. (1993) and Day et al. (1991). Data for the late cross-cutting quartz veins and the REE breccia pipe are more dispersed (+3.5 to +5.1), but are on average more positive (+4.2) than the earlier formed deposits (Fig. 3). The trend toward slightly more positive values with time for these deposits follows the trend toward more positive values in associated igneous rocks (the late cross-cutting dikes have an average ϵ_{Nd} of +5.5).

The coherence in the Nd isotope ratios across the region between Fe oxide mineralization and the igneous rocks supports a close relationship. There is a slight overlap in ϵ_{Nd} values between basement gneiss samples and the district-wide range

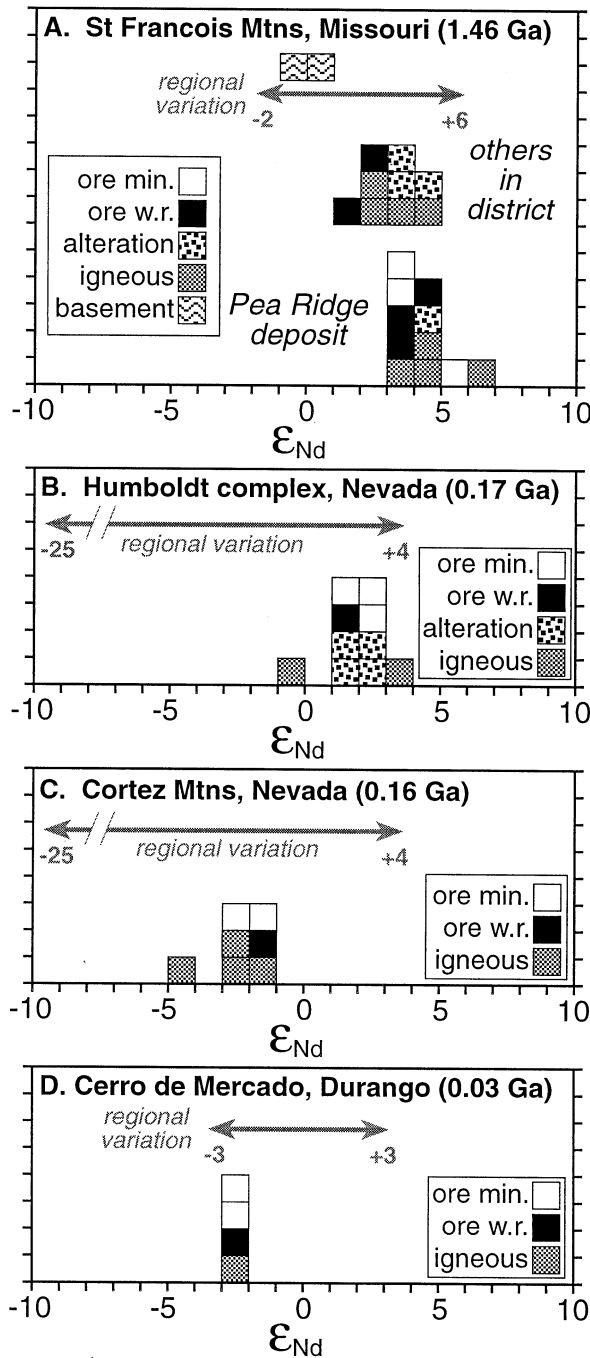


Fig. 2. Nd isotope histograms showing range of ϵ_{Nd} values for St. Francois Mountains (A), Humboldt mafic complex (B), Cortez Mountains (C), and Cerro de Mercado (D). Each system shows a relatively narrow range of Nd isotopic variation among the (generally) coeval igneous rocks, alteration assemblages, Fe oxide, and REE-bearing minerals. Also shown are ranges for $\epsilon_{Nd}(T)$ for other, generally older rocks in each region. The contemporaneous igneous host rocks overlap REE-enriched hydrothermal rocks in Nd isotopic composition in all cases, indicating dominantly igneous sources for the REE independent of age, setting, and type of igneous rock. Other sources cannot be precluded but show much larger spreads in their isotopic compositions than is observed in the hydrothermal systems.

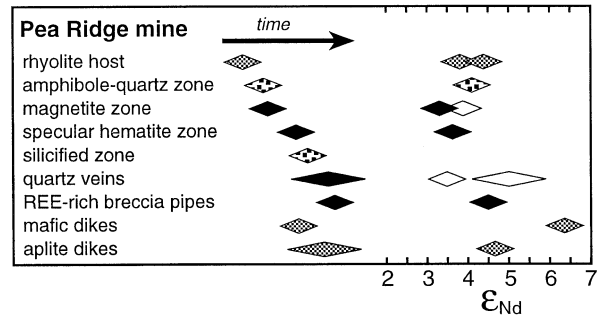


Fig. 3. Nd isotopic variations among coeval igneous rocks, Fe oxide replacement assemblages, and REE-rich deposits at the Pea Ridge Mine, Missouri, as a function of time (after Nuelle et al., 1992).

of isotopic compositions; however, the gneisses have ϵ_{Nd} values that fall well outside the range of the Pea Ridge data set (Fig. 2A). We note that Nelson and DePaolo (1985) and Bowring et al. (1991) obtained a somewhat smaller range of ϵ_{Nd} values than we did for the 1.49- to 1.44-Ga silicic igneous rocks of the St. Francois Mountains terrane (+4 to +5; on average slightly more positive than ours, but essentially identical to the REE deposits at Pea Ridge).

4.2. Humboldt Mafic Complex

Apatite mineral separates and associated Fe oxide minerals from the Humboldt Fe-P-REE deposits, along with a variety of fresh and altered host igneous rocks, were analyzed for their Nd isotopic composition (see Appendix 2 for sample descriptions and localities). The principal styles of mineralization in the Humboldt mafic complex include cross-cutting magnetite-apatite bodies, stratabound hematite bodies, and disseminated vein and breccia-controlled stockwork hematite-sulfide deposits (Reeves and Kral, 1955; Johnson et al., 1993). Cross-cutting relationships demonstrate that Fe oxide mineralization, alteration, and magmatism were broadly coeval. Most of the samples are from the area near the Buena Vista mine in the central part of the complex. In this tilted section, Jurassic volcanic and volcano-sedimentary rocks are intruded by a sheeted dike complex. The intrusive and volcanic rocks are altered to scapolite-dominated high temperature assemblages representing deep levels of hydrothermal alteration, and albite-dominated lower temperature assemblages representing shallower levels of hydrothermal alteration (Vanko and Bishop, 1982; Johnson

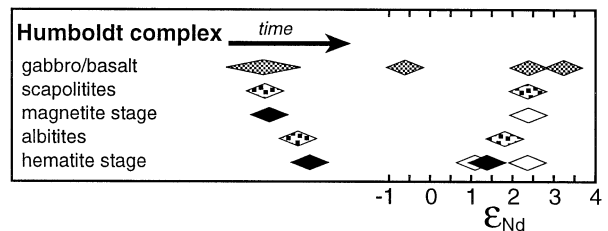


Fig. 4. Nd isotopic variations among coeval igneous rocks, Fe oxide replacement assemblages, and REE-rich minerals in the Buena Vista Mine area, Humboldt mafic complex, as a function of time (after Johnson, unpublished data).

et al., 1993). Magnetite-apatite assemblages occur at deeper levels as breccias, veins, and cross-cutting tabular bodies up to 10 m in width, which are cross-cut and partially replaced by albite-dominated assemblages containing intergrowths of calcite-apatite. Several generations of scapolitization have been recognized. Albitization is most abundant in the upper parts of the dike complex and overlying volcanic rocks, but albitized dikes also cross-cut scapolitized rock at depth. Stratabound specular hematite and pyrite deposits representing more distal, lower temperature parts of the hydrothermal system also occur at shallow levels throughout the overlying volcanic complex.

Sodically altered gabbroic and mafic volcanic rocks from the Buena Vista Mine area have ϵ_{Nd} ranging from +1.8 and +2.4 (Table 2; Fig. 2B). These include an albitized mafic dike (+1.8), which is part of a dike swarm cross-cutting intensely scapolitized gabbro in the deepest exposures at the Buena Vista Mine. Intensely scapolitized gabbroic rock representing the high temperature assemblage at the Buena Vista Mine has an ϵ_{Nd} of +2.4, whereas an albitized mafic volcanic rock from higher up in the volcanic pile above the main Fe oxide occurrences has an ϵ_{Nd} of +1.8. An albitized gabbro from the Cottonwood Canyon area, 15 km to the northeast where alteration is less intense, has an ϵ_{Nd} of +2.4. Fresh igneous lithologies are not available from the Buena Vista Mine area, but two gabbroic rocks from other parts of the complex have ϵ_{Nd} values of -1.0 (picritic basalt from the W. Humboldt Range) and +3.5 (unaltered gabbro from the Mopung Hills).

Apatite and associated Fe oxide deposits of the Humboldt mafic complex have ϵ_{Nd} values ranging from +2.4 to +1.1. In the Buena Vista Mine area, apatite from one of the early cross-cutting magnetite-apatite bodies has an ϵ_{Nd} = +2.4, identical to the scapolitized gabbro. Apatite from a late cross-cutting apatite-calcite vein has an ϵ_{Nd} of +2.3, whereas another apatite sample from the REE-rich outer rim of a zoned apatite crystal from another magnetite-apatite body yields an ϵ_{Nd} value of +1.1. A single sample analyzed from a stratabound hematite-rich zone associated with albitized volcanic rocks 6 km to the east in White Rock Canyon has an ϵ_{Nd} of +1.4.

Although igneous rocks display a larger range of isotopic variation than the hydrothermal Fe-P-REE deposits, the igneous rocks and mineralization have similar mean isotopic compositions (Table 1; Fig. 2B) compatible with a close relationship between the two. The isotopic compositions of early-formed high temperature assemblages at the Buena Vista Mine are quite homogeneous (ϵ_{Nd} = +2.4), with later samples showing a trend toward slightly more negative ϵ_{Nd} values with time (ϵ_{Nd} = +2.4 to +1.1; Fig. 4). It is possible that the REE sources for mineralizing fluids may have varied modestly from the early, high temperature assemblages to the later, low temperature assemblages in the more distal parts of the hydrothermal system. Overall, the isotopic composition of the Fe-P-REE deposits is uniform and within the range of associated igneous rocks.

4.3. Cortez Mountains

Nd isotopic compositions were measured for intrusive and volcanic rocks, their altered equivalents, and several stages of mineralization from the Cortez Mountains (see Appendix 2 for sample descriptions and localities). Jurassic quartz monzonitic and dioritic intrusions intrude and are overlain by a thick

sequence of Jurassic felsic volcanic rocks of the Pony Trail Group. The oldest rocks exposed are late Paleozoic sedimentary rocks. Sodic alteration of the intrusions and the lower Pony Trail Group is associated with widespread Fe oxide mineralization, along with potassic alteration restricted mainly to associated hypabyssal rocks and overlying volcanic rocks (Muffer, 1964; Johnson et al., 1993). Fe oxide bodies, consisting mainly of early magnetite-apatite overprinted by extensive hematitization, are typically discordant and range in size from a few meters in length to large, pipelike bodies more than 100 m across (Reeves et al., 1958). They are best exposed in the Frenchie Creek-Modarelli mine area, where large discordant bodies cut intensely altered volcanic rocks of the Pony Trail Group. Hematite and silica-rich assemblages replacing early magnetite-apatite also form independent bodies. At the Modarelli mine, hematite-cemented breccias containing clasts of magnetite-apatite rock are accompanied by specular and powdery hematite deposits. The breccias are cut by REE-rich jasperoidal siliceous breccias containing hematite and REE-bearing phosphate minerals. Nd isotopic values for the Cortez Mountains rock suite are significantly more negative than the Humboldt values (Table 2; Fig. 2C); however, overall isotopic trends between the two suites are similar. Fresh rhyolite, quartz monzonite, and diorite vary between ϵ_{Nd} = -2.0 and -4.4. Hydrothermal apatite from the Modarelli mine ranges from -2.4 (early apatite from magnetite-apatite rock) to ϵ_{Nd} = -2.0 (late apatite from a hematite-quartz-rich vein), whereas late-stage REE-rich siliceous mineralization has an ϵ_{Nd} of -1.7 (REE-rich jasperoidal breccia). Here, as at Humboldt, the Nd isotopic compositions of the Fe-P-REE deposits fall mostly the range of isotopic compositions for associated igneous rocks.

4.4. Cerro de Mercado

Four samples from the Cerro de Mercado district iron-oxide-apatite deposits yielded the same ϵ_{Nd} values (Table 2). Three samples were from Cerro de Mercado itself, one was from a nearby smaller deposit within the same part of the volcanic stratigraphy (the Mercado Iron Member of the Cacaria Formation; Lyons, 1988; see Appendix 2 for more complete sample descriptions). Two REE-rich apatite separates were analyzed. The first was from early-formed magnetite(martite)-apatite rock from the main ore body; the second was from late-formed apatite from typical late quartz cementing breccias in the massive iron oxides. The third sample, unaltered rhyolite, came from immediately outside the ore body. The fourth sample was from a layered hematite-gypsum deposit several kilometers away from Cerro de Mercado. The ϵ_{Nd} values range from -2.2 and -2.7, which are all within analytical uncertainty of the same mean value of -2.5 (Fig. 2D). These values are comparable to those found for other mid-Tertiary igneous rocks from this part of Mexico (ϵ_{Nd} +0.5 to -3).

5. DISCUSSION

The Nd isotopic data indicate that the REE contents in the Fe oxide-rich hydrothermal systems studied here are derived from the associated igneous rocks regardless of their age, geologic setting, and type. In the Nevada and Missouri deposits (this study), and in the Mesoproterozoic Olympic Dam deposit,

South Australia (Johnson and McCulloch, 1995), metasomatic rocks have more restricted ϵ_{Nd} than roughly time-equivalent igneous rocks and are far more restricted than regional crust. This relative uniformity is compatible with, but does not require, homogenization of REE from multiple igneous masses within the associated complexes. These isotopic results do not discriminate between alternative genetic models where aqueous fluids either originate from magmas or are derived from an external source and equilibrate with the crystallized equivalents. Either case would provide an igneous signature. Introduction of externally derived REE (e.g., country rock or basement sources, see Fig. 2) on a large scale is not evident, although such sources cannot be completely precluded given the isotopic heterogeneity in each region (cf. Farmer and DePaolo, 1997).

In the Humboldt, Cortez and Cerro de Mercado systems, nonmagmatic brines of likely evaporitic origin were involved as evidenced from local evaporites, sodium-metasomatism and stable isotope geochemistry (Vanko and Bishop, 1982; Battles and Barton, 1995; Barton and Johnson, 1996). Most interpretations of Pea Ridge and the other Missouri occurrences call on a magmatic fluid source to produce the high temperature brines recorded in these deposits (Day et al., 1991; Sidder et al., 1993); nonetheless, in this area there is regionally extensive oxygen isotope and alkali exchange that parallels changes seen in the other areas (Wenner and Taylor, 1976; Anderson, 1970). Although both magmatic and nonmagmatic fluids may have been involved in these systems, the common theme is that high salinities likely enhanced REE mobility. The high temperature experiments of Flynn and Burnham (1978) indicated REE complexing by chloride. Compatible with these results, Gammons et al. (1996) showed that complexing of Nd by Cl increases dramatically with temperature. Magmatic brines can carry their own REE inventory, whereas nonmagmatic brines could acquire REE by destruction of igneous apatite and other REE-bearing Ca minerals (e.g., titanite) during high temperature sodic alteration (Dilles and Einaudi, 1992; Johnson and Barton, 1997). This process can release REE into fluids that ultimately form early modestly REE-enriched hydrothermal apatite. Subsequently, destruction of early hydrothermal apatite at lower temperatures may further enrich REE as observed in late-formed apatites and other REE-rich phosphates (Johnson et al., 1995). More work, both experimental and field-based, is required before a sophisticated understanding can be obtained of REE mobilization and transport in these and other saline hydrothermal systems.

6. CONCLUSIONS

Nd isotopic data from REE-rich, Fe oxide-hosted igneous-related hydrothermal deposits of different ages, tectonic setting, and magmatic style in North America document the following: (1) initial Nd isotope ratios are similar in space and time for each system, (2) igneous rocks generally show greater Nd isotopic variation than REE-rich mineralization, and (3) there do not appear to be significant changes in REE sources between early and late stages of REE-rich mineralization. These observations lead us to conclude that, despite differences in the age, composition, and paragenesis of these Fe oxide deposits, the primary sources of REE in these systems are their coeval igneous rocks. Large-scale mobilization, homogenization, and

concentration of REE in hydrothermal Fe oxide deposits likely reflects a common oxidized, saline geochemistry that does not depend on associated igneous compositions, thus placing an independent constraint on the modes of origin.

Acknowledgments—This work was supported by the National Science Foundation (grants EAR 91-17372 and EAR 98-15032 to M.D.B.). We thank Jon Patchett for making his laboratory available for this work, and Lang Farmer and Warren Day for thoughtful reviews.

REFERENCES

- Anderson R. E. (1970) Ash-flow tuffs of Precambrian age in southeast Missouri. *Missouri Geol. Surv. & Water Res., Rept. Inv.* **46**.
- Barton M. D. and Johnson D. A. (1996) An evaporitic-source model for igneous-related Fe-oxide-(REE-Cu-Au-U) mineralization. *Geology* **24**, 259–262.
- Barton M. D. and Johnson D. A. (1997) A comparison of Fe-oxide (-Cu-Au-REE-U-Co-Ag) mineralization. *Geol. Soc. Am. Abstr. Progr.* **29**, 51.
- Barton M. D., Battles D. A., Bebout G. E., Capo R. C., Christensen J. N., Davis S. R., Hanson R. B., Michelsen C. J., and Trim H. E. (1988) Mesozoic contact metamorphism in the western United States. In *Metamorphism and Crustal Evolution, Western Conterminous United States* (ed. W. G. Ernst), Rubey Volume VII, pp. 110–178, Prentice-Hall.
- Barton M. D., Marikos M. A., and Johnson D. A. (1993) A comparison of felsic and mafic Fe-P-(REE-Cu) Deposits. *Geol. Soc. Am. Abstr. Progr.* **25**, 5.
- Battles D. A. and Barton M. D. (1995) Arc-related sodic hydrothermal alteration in the western U.S. *Geology* **23**, 913–916.
- Bowring S. A., Housh T. B., and Podosek F. A. (1991) Nd isotopic constraints on the evolution of Precambrian “anorogenic” granites from Missouri. *EOS* **72**, 310.
- Day W. C., Sidder G. B., Rye R. O., Nuelle L. M., and Kisvarsanyi E. B. (1991) The Middle Proterozoic rhyolite-hosted Pea Ridge iron and rare-earth-element deposit: A magmatic source for Olympic Dam-type deposits in the Midcontinent region of the U.S.A. In *Second Hutton Symposium on Granites and Related Rocks* (ed. B. W. Chappell), p. 409.
- Dilles J. H. and Einaudi M. T. (1992) Wall-rock alteration and hydrothermal flow paths about the Ann-Mason porphyry copper deposit, Nevada: A 6-km vertical reconstruction. *Economic Geology* **87**, 1963–2001.
- Einaudi M. T. and Oreskes N. (1990) Progress toward an occurrence model for Proterozoic iron oxide deposits—A comparison between the ore provinces of South Australia and Southeast Missouri. *U.S. Geol. Surv. Bull.* **1932**, 58–69.
- Emery J. A. (1968) Geology of the Pea Ridge iron ore body. In *Ore Deposits of the United States, 1933–1967* (ed. J. Ridge), V. 1, pp. 359–369, Am. Inst. Mining, Metall. and Petroleum Engineers.
- Farmer G. L. and DePaolo D. P. (1997) Sources of hydrothermal components: Heavy isotopes. In *Geochemistry of Hydrothermal Ore Deposits* (ed. H. L. Barnes), 3rd ed., pp. 31–62. Wiley and Sons.
- Flynn R. T. and Burnham C. W. (1978) An experimental determination of rare earth partition coefficients between a chloride containing vapor phase and silicate melts. *Geochim. Cosmochim. Acta* **42**, 685–702.
- Foose M. P. and McLelland J. M. (1995) Proterozoic low-Ti iron-oxide deposits in New York and New Jersey: Relation to Fe-oxide (Cu-U-Au-rare earth element) deposits and tectonic implications. *Geology* **23**, 665–668.
- Frietsch R. and Perdahl J. A. (1995) Rare earth elements in apatite and magnetite in Kiruna-type iron ores and some other iron ore types. *Ore Geol. Rev.* **9**, 489–510.
- Gammons C. H., Wood S. A., and Williams-Jones A. E. (1996) The aqueous geochemistry of rare earth elements and yttrium: VI. Stability of neodymium chloride complexes from 25 to 300 degrees C. *Geochim. Cosmochim. Acta* **60**, 4615–4630.
- Gow P. A., Wall V. J., Oliver N. H. S., and Valenta R. K. (1994) Proterozoic iron oxide (Cu-U-Au-REE) deposits: Further evidence of hydrothermal origins. *Geology* **22**, 633–636.

- Haynes D. W., Cross K. C., Bills, R. T., and Reed, M. H. (1995) Olympic Dam ore genesis: A fluid-mixing model. *Economic Geology* **90**, 281–307.
- Hitzman M. W., Oreskes N., and Einaudi M. T. (1992) Geological characteristics and tectonic setting of Proterozoic iron oxide (Cu-U-Au-REE) deposits. *Precambrian Res.* **58**, 241–287.
- Husman J. R. (1989). Gold, rare earth element, and other potential by-products of the Pea Ridge iron ore mine, Washington County, Missouri. *Missouri Div. Geol. Land Surv., Open-File Report OFR-89-78-MR*.
- Johnson D. A. and Barton, M. D. (1997) *Mass-balance relationships in iron-oxide(-copper-rare-earth-element) deposits in the Great Basin*. Seventh Annual V. M. Goldschmidt Conference, p. 108, LPI Contribution No. 921, Lunar and Planetary Institute.
- Johnson D. A., Barton M. D., and Hassanzadeh, J. (1993) Mafic and felsic hosted Fe-apatite-(REE-Cu) mineralization in Nevada. *Geol. Soc. Am. Abstr. Progr.* **25**, 57.
- Johnson D. A., McCandless T. E., Ruiz J., and Barton M. D. (1995) Rare earth elements in apatite by laser ablation ICP-MS: Implications for Fe-(P-REE-Cu) mineralization in Kiruna-type systems. *EOS* **76**, 287.
- Johnson J. P. and Cross K. C. (1991) Geochronological and Sm-Nd isotopic constraints on the genesis of the Olympic Dam Cu-U-Au-Ag deposit, South Australia. In *Source, Transport, and Deposition of Metals* (eds. M. Pagel and J. L. Leroy), pp. 395–400, Balkema.
- Johnson J. P. and McCulloch M. T. (1995) Sources of mineralising fluids for the Olympic Dam deposit (South Australia): Sm-Nd isotopic constraints. *Chemical Geology* **121**, 177–199.
- Kisvarsanyi E. B. (1990) General features of the St. Francis and Spavinaw granite-rhyolite terranes and the Precambrian metallogenic region of southeast Missouri. *U.S. Geol. Surv. Bull.* **1932**, 48–57.
- Kisvarsanyi G. and Kisvarsanyi E. B. (1981). Genetic relationship of Kiruna-type apatitic iron ores to magnetite trachyte and syenite in the St. Francois Terrane, Missouri. *Geol. Soc. Am. Abstr. Progr.* **13**, 488.
- Kisvarsanyi G. and Smith F. J. (1988). Boss-Bixby, a high temperature iron-copper deposit in the Precambrian of the midcontinent United States. *Missouri Div. Geol. Land Surv., Open-File Report OFR-88-72-GI*.
- Labarthe-Hernandez I. G., Tristan Gonzalez I. M., and Aguillon Robles I. A. (1987) Analisis de la Mina Cerro del Mercado, Dgo. *Geomimet* **151**, 2–14.
- Lyons J. I. (1988) Volcanogenic iron oxide deposits, Cerro de Mercado and vicinity, Durango, Mexico. *Econ. Geol.* **83**, 1886–1906.
- Marikos M. A. and Barton M. D. (1993) Sm-Nd and Rb-Sr systematics of the Pea Ridge Fe-P deposit and related rocks, southeast Missouri. *Geol. Soc. Am. Abstr. Progr.* **25**, 65.
- Marikos M. A., Nuelle, L. M., and Seeger C. M. (1990) Geologic mapping and evaluation of the Pea Ridge iron ore mine (Washington County, Missouri) for rare earth element and precious metals potential—A progress report. *U.S. Geol. Surv. Bull.* **1932**, 76–81.
- Muffler L. J. P. (1964) Geology of the Frenchie Creek quadrangle north-central Nevada. *U.S. Geol. Surv. Bull.* **1179**, 99 p.
- Nelson B. R. and DePaolo D. J. (1985) Rapid production of continental crust 1.7–1.9 b.y. ago: Nd isotopic evidence from the basement of the North American mid-continent. *Geol. Soc. Amer. Bull.* **96**, 746–754.
- Nuelle L. M., Day W. C., Sidder G. B., and Seeger C. M. (1992) Geology and mineral paragenesis of the Pea Ridge iron ore mine, Washington County, Missouri—Origin of the rare-earth-element and gold-bearing breccia pipes. *U.S. Geol. Surv. Bull.* **1989**, A1–A11.
- Oreskes N. and Einaudi M. T. (1990) Origin of rare earth element-enriched hematite breccias at the Olympic Dam Cu-U-Au-Ag deposit, Roxby Downs, South Australia. *Econ. Geol.* **85**, 1–28.
- Patchett P. J. and Ruiz J. (1987) Nd isotopic ages of crust formation and metamorphism in the Precambrian of eastern and southern Mexico. *Contr. Min. Pet.* **96**, 523–528.
- Reeves R. G. and Kral V. E. (1955) Iron ore deposits of Nevada. Part A, Geology and iron ore deposits of the Buena Vista Hills, Churchill and Pershing Counties, Nevada. *Nevada Bur. Mines Bull.* **53**, 32p.
- Reeves R. G., Shawe F. R., and Kral V. E. (1958) Iron ore deposits of Nevada. Part B, Iron ore deposits of west-central Nevada. *Nevada Bur. Mines Bull.* **53**, 78 p.
- Seeger C. M., Nuelle L. M., and Marikos M. A. (1989) Massive silicification and late stage quartz veining in the Pea Ridge Fe-REE deposit, southeast Missouri. *Geol. Soc. Am. Abstr. Progr.* **21**, 34.
- Sidder G. B., Day W. C., Nuelle L. M., Seeger C. M., and Kisvarsanyi E. B. (1993) Mineralogic and fluid-inclusion studies of the Pea Ridge iron-rare-earth-element deposit, southeast Missouri. *U.S. Geol. Surv. Bull.* **2039**, 205–216.
- Sims P. K. (1990) Geologic setting and ages of Proterozoic anorogenic rhyolite-granite terranes in the central United States. *U.S. Geol. Surv. Bull.* **1932**, 40–47.
- Speed R. C. (1976) Geologic map of the Humboldt lopolith and surrounding terrane, Nevada. *Geol. Soc. Am. Map Chart and Series MC-14*.
- Van Schmus W. R., Bickford M. E., and Turek A. (1996) Proterozoic geology of the east-central midcontinent basement. *Geol. Soc. Am. Spec. Pap.* **308**, 7–32.
- Vanko D. A. and Bishop F. C. (1982) Occurrence and origin of marialitic scapolite in the Humboldt Lopolith, N.W. Nevada. *Contr. Min. Petrol.* **81**, 277–289.
- Wenner D. B. and Taylor H. P. (1976) Oxygen and hydrogen isotope studies of a Precambrian granite-rhyolite terrane, St. Francois Mountains, southeastern Missouri. *Geol. Soc. Am. Bull.* **87**, 1587–1598.

Appendix 1. Sample localities and descriptions for St. Francois Mountains, southeast Missouri.

Sample no.	Material	Description	Location
88FT920	Magnetite trachyte ^a	Porphyritic texture with sauseritized plagioclase phenocrysts in dark gray to black-brown microcrystalline groundmass of quartz and K-feldspar. Magnetite dust and clots permeate the groundmass.	Missouri, Floyd Tower; 37°58'53.2"N, 90°58'38.8"W
WA11-1256	Trachy-basalt ^a	Remnant plagioclase phenocrysts in gray-black microcrystalline groundmass of K-feldspar and quartz with ubiquitous magnetite dust and clots. Small radiating blue-green amphibole sprays cut across groundmass and phenocrysts.	Missouri, Floyd Tower; 38°03'28.4"N, 90°52'35.6"W
88PR020	Aplite dike ^b	Fine-grained orange aplitic dike-rock with sub-equal portions of quartz and K-feldspar and minor muscovite. Traces of rutile as polysynthetic twins.	Missouri, Pea Ridge Mine; 38°07'30.0"N, 91°02'45.6"W
88PR26	Hematite with minor quartz	Massive specular hematite from 2275 level, X11 drift (see Nuelle et al., 1991, Fig. A3)	Missouri, Pea Ridge Mine; 38°07'30.0"N, 91°02'45.6"W
88PR118	Xenotime	Clear honey-colored dipyrimal prisms from late quartz veins.	Missouri, Pea Ridge Mine; 38°07'30.0"N, 91°02'45.6"W
88PR120	Late apatite	Clear yellow euhedra from late quartz veins.	Missouri, Pea Ridge Mine; 38°07'30.0"N, 91°02'45.6"W
88PR999	Early apatite	Milky pink to brown euhedra contemporaneous with actinolite near footwall of magnetite body.	Missouri, Pea Ridge Mine; 38°07'30.0"N, 91°02'45.6"W
90PR004	Mafic dike ^b	Fine-grained gray-green dike-rock with white plagioclase laths and chloritized pyroxene.	Missouri, Pea Ridge Mine; 38°07'30.0"N, 91°02'45.6"W
90PR12	Quartz-amphibole rock ^b	From high-grade magnetite ore from interior of orebody.	Missouri, Pea Ridge Mine; 38°07'30.0"N, 91°02'45.6"W
90PR23	Massive ore	Coarse-grained ferroactinolite, quartz, biotite, magnetite, pyrite rock near footwall of magnetite body.	Missouri, Pea Ridge Mine; 38°07'30.0"N, 91°02'45.6"W
90PR44	Black porphyry ^c	Porphyritic flow with pink K-feldspar laths and fresh elongate hornblende phenocrysts in brown-black glassy groundmass.	Missouri, Pea Ridge Mine; 38°07'30.0"N, 91°02'45.6"W
90PR52	2275 Porphyry ^b	Brick-red volcanic rock with large K-feldspar phenocrysts in fine groundmass dominated by quartz and minor K-feldspar. Shows signs of extensive silicification of groundmass and phenocrysts.	Missouri, Pea Ridge Mine; 38°07'30.0"N, 91°02'45.6"W
90PR53	Breccia pipe fill	Soft friable rock of K-feldspar, barite, and chlorite. High U, Th, and REE content due to fine-grained monazite and xenotime.	Missouri, Pea Ridge Mine; 38°07'30.0"N, 91°02'45.6"W
93IMA	Amphibole separate	From dump sample with coarse compact actinolite radiating from fracture wall. Interior of vein filled with massive hematite.	Missouri, Iron Mountain Mine; 37°41'53.4"N, 90°38'13.8"W
93IMG	Garnet separate	Fine-grained yellow-brown zoned andradite garnet after actinolite.	Missouri, Iron Mountain Mine; 37°41'53.4"N, 90°38'13.8"W
IM3948	Andesite dike	Very fine-grained gray-green dike rock containing plagioclase and chloritized hornblende.	Missouri, Iron Mountain Mine; 37°41'53.4"N, 90°38'13.8"W
J17SILL	Granite sill	Coarse-grained orange granite with K-feldspar, quartz, biotite cutting orebody and altered rocks.	Missouri, Boss-Bixby Mine; 38°26'52.8"N, 91°10'45.1"W
J17SYEN	Boss-Bixby "Syenite"	Dark gray-black fine-grained K-feldspar, quartz rock with abundant magnetite. ^d	Missouri, Boss-Bixby Mine; 38°26'52.8"N, 91°10'45.1"W
L3-1713	Paragneiss	Sillimanite-muscovite-biotite gneiss from subsurface. ^e	Missouri, Lawrence County; 38°37'11.3"N, 90°37'59.9"W
GE1	Orthogneiss	Granodiorite gneiss from subsurface. ^e	Missouri, Gentry County; 40°10'48.0"N, 94°24'36.0"W
PKPIPE	Breccia pipe fill	Massive orange to tan K-feldspar, quartz and barite rock with remnant breccia-texture from underground mine.	Missouri, Pilot Knob; 37°37'11.2"N, 90°38'0.0"W
PKSURF	Bedded hematite	Bedded hematite, quartz, K-feldspar rock showing delicately preserved graded bedding, ripples and mud-cracks. From surface mine.	Missouri, Pilot Knob; 37°37'10.2"N, 90°37'25.0"W

^a Kisvarsanyi and Kisvarsanyi (1981).^b Emery (1968).^c Husman (1989).^d Kisvarsanyi and Smith (1988).^e Van Schmus et al. (1996).

Appendix 2. Sample localities and descriptions for Humboldt mafic complex and Cortez Mountains, western and central Nevada, and Cerro de Mercado, Durango, Mexico.

Sample ID	Material	Description	Location
<i>Cortez Mountains</i>			
CM90-1g'	Jasperoid	REE-rich jasperoid from late silica-rich assemblage; consists of silica + hematite \pm limonite group minerals and monazite; crosscuts massive iron oxide	Modarelli mine (bench 5); 116°15.7'N, 40°22'W
CM90-1a	Rhyolite	White rhyolite consisting of K-feldspar, plagioclase, quartz, minor biotite; weakly hydrolytic alteration: biotite, feldspars partly converted to hematite and sericite/clays, respectively	Modarelli mine/Frenchie Creek area; 116°16.5'N, 40°21.6'W
CM92-03f	Granite	From late hypabyssal granite stock; consists of equigranular quartz, K-feldspar, plagioclase, amphibole, biotite, minor magnetite; intrudes Frenchie Creek Rhyolite	Frenchie Creek/Sod House Creek area; 116°20.8'N, 40°22'W
CM92-04a	Diorite	Early intruded diorite of the Duff Creek pluton; seriate texture, zoned plagioclase, clinopyroxene. ^a	Mouth of Duff Creek, south side; 116°23.3'N, 40°20.3'W
CM92-06p	Apatite	From apatite-hematite-martite vein cutting Frenchie Creek rhyolite; distal/late iron-oxide assemblage	Modarelli mine bench (10); 116°15.8'N, 40°22'W
CM92-01g	Latite	Lowest unit of Frenchie Creek Rhyolite; tan with 5 vol.% phenocrysts (K-feldspar plagioclase, biotite, 4 vol.% magnetite) fresh feldspars; biotite edges oxidized to hematite	Pony Trail Canyon; 116°15.3'N, 40°22.6'W
CM92-06m	Apatite	Earlier formed massive apatite-martite with later silica overgrowths	Modarelli mine (bench 10); 116°15.8'N, 40°22'W
<i>Cerro de Mercado, Durango</i>			
D93-3n'	Apatite	Apple green apatite from late-stage apatite-silica assemblage, overgrowing magnetite (martite)	Cerro de Mercado mine (block along ramp leading into pit)
D93-3a	Apatite	Early-formed apatite intergrown with magnetite (martite) and minor pyroxene	Cerro de Mercado mine (at N end of pit)
D93-4a	Rhyolite	Pink welded rhyolitic tuff from Carpintero Group (Santuario Fm); 2 vol.% phenocrysts composed of K-feldspar, plagioclase, minor biotite phenocrysts (<0.5%); feldspars fresh in glassy, hard groundmass	Roadcut along highway 40, west of Durango
D93-4t	Gypsum/hematite	Stratabound, interbedded gypsum and hematite; overlies altered rhyolite and may be distal facies of massive, stratabound fine-grained hematite	El Mulato prospects, west of city of Durango, north of highway 40
<i>Humboldt Complex</i>			
Hm91-G-Ap	Apatite	Large, light green, apatite crystals, 5 cm long; in late calcite filled vugs, probably same as late calcite-apatite-actinolite-titanite-magnetite-albite assemblage; fills vugs in massive magnetite-apatite	Buena Vista Hills, Magnetite prospect 6 miles northeast of main pit; 118°9.7'N, 39°58.6'W
Hm92-6h	Olivine cumulate ("picrite") ^b	Olivine orthocumulate from a small sheet; up to 4 cm tabular plagioclase forms igneous foliation; cumulate minerals include euhedral to subhedral olivine, large euhedral plagioclase, clinopyroxene	Southern picrite body in West Humboldt Range; 118°23.0'N, 40°1.6'W
Hm94-1g	Albitized mafic volcanic rock	Strongly albitized mafic volcanic rock with feldspar phenocrysts; groundmass replaced by albite and ankeritic dolomite, with minor titanite and apatite	1.2 miles SE of Buena Vista Mine pit, Buena Vista Hills; 118°8.5'N, 39°58.25'W
Hm93-11a'	Weakly altered gabbro	Equigranular, medium-grained gabbro composed of plagioclase, clinopyroxene, pargasitic hornblende, minor ilmenite, apatite, and magnetite; feldspars are partly replaced by sericite, chlorite, minor epidote	Gabbroic outcrops along road near pass in Mopung Hills, southern tip of West Humboldt Range; 118°42.0'N, 39°53'W
Hm93-16t	Hematite-silica	Bedded, fine-grained specular hematite and silica (small-scale folding common suggestive of soft sediment deformation).	Outcrop along upper west branch of White Rock Canyon, Stillwater Range; 118°3.57'N, 39°56.63'W
TrJ89-6b	Weakly altered gabbro	Equigranular gabbro (plagioclase, clinopyroxene, amphibole, and minor biotite, ilmenite, magnetite, apatite), feldspars rimmed by early scapolite-albite and partially replaced by chlorite, epidote	Lower Cottonwood Canyon, outcrop 1.2 mile up stream from mouth of canyon, Stillwater Range; 117°53.25'N, 40°58.8'W
TrJ89-7c	Scapolitized mafic rock	White, coarse-grained scapolitite	White outcrops 100 m north of pit, Buena Vista Mine, Buena Vista Hills; 118°10.25'N, 39°58.4'W
TrJ89-7f	Apatite	Massive magnetite-apatite-hornblende-chlorite-titanite ore, early assemblage	From main pit at Buena Vista Mine, Southern Buena Vista Hills; 118°10.1'N, 39°58.4'W
TrJ90-1c	Apatite	Large (>10 cm) light green apatite crystals; from late calcite-apatite-actinolite-titanite \pm magnetite \pm albite rocks; occurs as vugs and vein fillings within and crosscutting massive earlier magnetite-apatite assemblage	From main pit at Buena Vista Mine, Southern Buena Vista Hills; 118°10.1'N, 39°58.4'W
TrJ90-13a	Albitized mafic dike	Late-stage, strongly albitized mafic dike, crosscutting strongly scapolitized rock; albite and minor carbonate replacing feldspars; mafic minerals replaced by hydrothermal actinolite, clinopyroxene, and chlorite	From small white hill 1/2 mile north of main pit at Buena Vista Mine, Southern Buena Vista Hills; 118°10.25'N, 39°58.9'W

^a Muffler (1964).^b Speed (1976).